Thermodynamics and fragility of glass-forming alloys

(Article begins on next page)

15 July 2024

Thermodynamics and fragility of glass-forming alloys

L. Battezzati* and G. Dalla Fontana

Dipartimento di Chimica e Centro NIS, Università di Torino, Via P. Giuria 7, 10125 Torino, Italy

Corresponding Author: livio.battezzati@unito.it, tel 0039 011 6707567, fax 0039 011 6707855.

Abstract

The existing correlation between the extensive properties, ΔH and ΔS, the enthalpy and entropy difference between liquid and crystal phases has been checked to relate metallic glasses to other classes of amorphous materials.

Expressing the specific heat difference, ΔC_p, of molten and crystalline metallic glass-formers as a function of temperature with different functional trends, parametric expressions of fragility are derived using relevant temperatures for alloys. It is shown that relationships between the $\Delta S_g/\Delta C_{p,g}$ ratio and such temperatures are useful to estimate unknown quantities when the experimental determination of the specific heat is possible.

Thermodynamic indicators of fragility are compared to the kinetic fragility obtained from viscosity data accounting for the estimated errors on parameters which are derived from extrapolations. The outcome of the analysis indicates that a relationship between thermodynamic and kinetic parameters exists. Moreover a systematic scatter for some alloys indicates a diverse behaviour which can be ascribed to structure modification either in the liquid or in the solid reference state.

1. Introduction

Since the early times of rapid solidification processing, the formation of metallic glasses from a supercooled melt near deep eutectics showed that it is necessary to meet specific thermodynamic conditions, in addition to a proper quenching technique, to allow survival of the liquid at low temperatures and transform it into a glass.

These requirements are expressed by the trend of extensive properties, ΔH and ΔS, the enthalpy and entropy difference between liquid and crystal phases which, obviously, will determine the trend of ΔG, the related difference in free energy [1]. The functional form of these quantities versus temperature depends on the specific heat of the liquid and of the solid (C_p^l and C_p^s). While the solid specific heat complies to the rule of mixing molar quantities of the elements, the specific heat of the liquid deviates considerably from it having an increasing trend on decreasing temperature. The Potential Energy Landscape (PEL) model suggests this is due to sampling of a varied number of potential energy minima among the vast ensemble of them available in the liquid at every temperature [2]. As a consequence, it might be envisaged the C_p^l curves could be used to study the so-called melt thermodynamic fragility. This concept has been introduced by expressing the rate of entropy loss in the temperature range of the glass transition: a faster rate of entropy loss implies a more rapid change in the number of states sampled by the liquid, therefore termed fragile in contrast to the strong ones having less states available and, consequently, more steady dependence on temperature of entropy [2]. Application of the PEL model has provided insight also into the dynamics of liquids, e. g. structural relaxation times and viscosity, which is equally controlled by the landscape topology showing a correlation between kinetic and thermodynamic properties of glass-formers [3].

Following up an extensive discussion on the specific heat behaviour of metallic glass formers in relation to fragility indicators [4], in this paper we discuss first the correlation between thermodynamic quantities, then we check for simple correlations between thermodynamic and kinetic properties of metallic glass-formers and compare them with those of other melts both

inorganic and organic. The aim is to provide a general frame of "normal" behaviour, possibly usable to estimate quantities for new alloys, and, eventually, find exceptions worth of further investigation in terms of structure of the liquid and of possible transformations of it in the undercooling regime.

2. Correlation between thermodynamic quantities of undercooled melts

The extensive thermodynamic properties of a substance as a function of temperature are correlated. according to the respective dependence on the specific heat [1].

$$\frac{\Delta S_g}{\Delta S_m} \Bigg/ \frac{\Delta H_g}{\Delta H_m} = (1 - \int_{T_g}^{T_m} \frac{\Delta C_p}{\Delta S_m} d\ln T) \Bigg/ (1 - \int_{T_g}^{T_m} \frac{\Delta C_p}{\Delta H_m} dT) \qquad (1)$$

For glass-forming alloys the liquid specific heat is higher than that of the corresponding solid. This behaviour is actually general for all classes of glass-formers and leads to enthalpy and entropy loss on undercooling with an envisaged catastrophe when the property equals that of the solid. The long-standing Kauzmann paradox refers to such entropy crisis at the temperature T_K which is avoided by vitrifying the melt at a glass transition temperature, T_g, kinetically defined [5]. At this temperature the extensive thermodynamic quantities are frozen-in with values which can be computed if the specific heat and melting enthalpy of the substance are known from calorimetry measurements. With this in mind it is of interest to exploit the links between properties to estimate the value or range of those which are not amenable to measurement, e. g. the amount of entropy frozen-in at the glass transition.

With the discovery of bulk glass-formers in various alloy systems, data on transition temperatures, heat of fusion and specific heat are now available in the literature. Their quality and scatter has been thoroughly discussed earlier [4] motivating a critical selection of data on metallic glasses based on Zr, La, Pd, Cu, Mg, Au and Pt.

The relevant compositions are reported in Tab. 1. For simplicity, in the following graphs each alloy listed in Tab. 1 will be identified only by means of the base element and/or the corresponding number.

For these alloys Fig. 1 shows the correlation between ΔS_g, the entropy of the liquid frozen-in at the glass transition temperature and the corresponding enthalpy content, ΔH_g, with both quantities referred to the respective value at the melting (eutectic) point ΔS_m and ΔH_m. The bisector line in the figure corresponds to the case of the difference in specific heat between liquid and crystal phases, ΔC_p, being nil as reported for some pure elements, at least at high temperature. The area above the bisector line corresponds to the rather unphysical case $\Delta C_p < 0$. The points referring to metallic glass-formers cluster in between two limiting lines which were computed by assuming an hyperbolic dependence of ΔC_p on temperature between T_m and T_g and a T_g/T_m ratio of ½ and 2/3 expressing the cases for either marginal or good glass-formers, respectively [26]. Should ΔC_p be expressed by other functions (e. g. linear, T^{-2}) lines could be drawn falling very close to these. It should also be noted that the inevitable error in the experimental determination of ΔC_p versus temperature will affect ΔS and ΔH in the same sense because of the correlation expressed by eq.1, but their ratio to a minor extent. In the event that T_g is close to the crystallization temperature of the glass, T_x, i. e. the materials is a marginal glass-former, the experimental determination of the enthalpy of crystallization, ΔH_x, will allow the estimate of the residual entropy at the same temperature by using the relative correlation line.

3. The residual entropy at T_g and fragility parameters

The quantity ΔS_g has been thoroughly discussed in the literature on the glass transition. It was suggested at first it should take a "universal" value if expressed per mole of bead, i. e. an appropriate structural unit to be defined by examining the structure of the material. It appeared, however, that this would not hold for substances of different families where diverse contributions to

the total residual entropy could appear and be relevant. This was inferred from the location of points referring to various substances in a plot of ΔS_g versus $\ln(T_g/T_K)$ [27] where several correlation lines were drawn each implying a constant, or effective, value of ΔC_p in the temperature range between T_g and T_K[1]. In this context, metallic glasses, for which a "bead" should correspond to every atom in the alloy, appear to align similarly to inorganic glasses, with slope of $\Delta C_p = 18$ J/mol·K, higher than that of polymeric and organic glasses (12.5 J/mol·K) (Fig. 2).

The concept of "bead" has been recently re-used to define the units for molecular motion in the description of the library of possible states in the potential energy landscape (PEL) of the undercooled melt [26, 28] The distribution in energy of such states for "excitable units" in the PEL has been modelled as gaussian, hyperbolic, and logarithmic[3] establishing links between the configurational entropy content of the melt and its dynamic properties, especially viscosity. This connection implies that the viscosity diverges at a temperature $T_0 = T_K$, being expressed by the Vogel-Fulcher-Tammann equation [29]

$$\eta = \eta_\infty \exp(\frac{B}{T - T_0}) \tag{3}$$

where η_∞ gives the viscosity in the high temperature limit, $B = DT_0$ contains information on the fragility, D.

It has been argued that T_0 and T_K do not coincide and the latter temperature exceeds the former in dependence of the fragility parameter, m [26],

$$m = \left[\frac{d\log(\eta)}{d\frac{T_g}{T}} \right]_{T=T_g}. \tag{4}$$

In Fig. 3 the T_K/T_0 ratio is plotted versus m [7] for metallic glasses and the substances, mostly organic, listed in the Table available online [26]. Although on average the points actually lie above unity, no clear trend is discernible. At present, it cannot be stated with certainty whether this

---

[1] The plot stems from $\Delta S_K = 0 = \Delta S_g - \Delta C_p \ln(T_g/T_K)$. (2)

expresses a departure from the common assumption that $T_K = T_0$, considering also the deviation associated to both temperatures (see the estimated scatter of the ordinate) which are obtained by extrapolation of either the entropy or the viscosity to ranges where experiments cannot provide direct measurement of properties.

The early assumption of a constant value of ΔC_p in the temperature range between T_g and T_K appears limiting to date also in view of the models of the number of states in the PEL which are constructed by taking ΔC_p dependent on temperature as T^{-n} with n of order 1 and 2 [26]. With n = 1, the modified relationship (with respect to that expressed by Fig. 2) is expressed by

$$\frac{\Delta S_g}{\Delta C_{p,g}} = \frac{T_g - T_K}{T_K} \tag{5}$$

as shown in Fig. 4. The correlation appears enhanced in comparison to Fig. 2. Here again the *caveat* holds, as stated above, on the error in determining ΔC_p versus temperature which affects both ΔS_g and T_K. In spite of this, should ΔS_g, $\Delta C_{p,g}$ and T_g be known from independent experiments or calculations, T_K could be estimated from the plot.

The left hand side of eq. 5 is the inverse of the exact expression of the thermodynamic fragility parameter, m_T [26, 3], defined as:

$$m_T = \left[\frac{d \dfrac{\Delta S_g}{\Delta S}}{d \dfrac{T_g}{T}} \right]_{T=T_g} \tag{6}.$$

Assuming an hyperbolic distribution of the states in the PEL of the melt, it was derived that

$m_T + 1 = \dfrac{m}{17} = \dfrac{T_g}{T_g - T_K}$, therefore the right hand side (rhs) of eq. 5 equals *1/(m_T-1)*. Fig. 4 results then

a representation of the melt fragility within such assumption.

A parallel conclusion is obtained by assuming n = 2 and obtaining

$$\frac{\Delta S_g}{\Delta C_{p,g}} = \frac{T_g^2 - T_K^2}{T_K^2} \qquad (7)$$

In this case the rhs of eq. 7 becomes $1/(m_T-1)$ when it is posed $m_T + 1 = \dfrac{T_g^2 + T_K^2}{T_g^2 - T_K^2}$ [3], as a consequence of assuming a gaussian distribution of the states in the PEL of the melt. The corresponding plot does not add information with respect to the previous one and is not reported here.

4. Link with kinetic fragility parameters

Analyzing in detail the values of the quantities reported in Fig. 4 it appears that some $\Delta S_g/\Delta C_{p,g}$ ratios are irrealistically too low, or that some $\Delta C_{p,g}$'s are too high for an undercooled liquid phase. This is likely due to extrapolation of high temperature data to the inaccessible range. For the sake of comparison, although with the warning of the deviation shown in Fig, 3, an analogous plot as been constructed by substituting the T_0 obtained by fitting viscosity data for T_K (Fig. 5). As expected, the scatter of point is large, although a correlation is still recognized. It is seen that most of the points just mentioned are displaced with respect to the correlation line. Others fall clearly off any conceivable correlation suggesting that the data should be reconsidered, possibly with new and more extended experiments. A further hint in this sense will be given at the end of this paragraph.

The T_0 temperature is also derived from data extrapolation and therefore carries a substantial uncertainty. It, however, has been shown to correlate rather nicely with the *B* parameter [13] in eq. 3. Since the pre-exponential factor of viscosity is of the order of 10^{-5} Pa·s in most cases and the viscosity at T_g is conventionally taken as 10^{12} Pa·s, the *B* and T_0 parameters are related by $\ln 17 = B/(T_g - T_0)$. This is confirmed for the ensemble of alloys examined in this work by the plot of Fig. 6. In the event that the viscosity can be expressed by eq. 3, the dynamic fragility parameter *m* defined in eq. 4 is given by

$$m = BT_g \big/ \big[2.3(T_g - T_0)^2 \big] \qquad\qquad (8)$$

and, therefore, the knowledge derived from either experiments or calculation, of any of the m, B, and T_0 parameters will allow deriving the others.

An empirical formula [26] to compute m using thermodynamic quantities accessible to experiments has proved rather accurate for various inorganic and organic substances

$$m = 56 \frac{T_g \Delta C_{p,g}}{\Delta H_m} \qquad\qquad (9).$$

Application of eq. 9 to metallic glasses shows that the general trend is followed, although with large scatter especially for some compositions (Fig. 7). The deviation from the mainstream behaviour appear useful, however, to pinpoint materials for which the above formula is not applicable either because of scatter in the experimental data or, more interestingly, because of inherent structural modifications: e. g. a ring-chain equilibrium in the liquid state of sulphur and selenium gives an extra contribution to the specific heat of the melt which is not accounted for in eq. 9. In the case of metallic glasses the largest deviation is for the $Au_{77}Ge_{13.6}Si_{19.4}$ glass-forming melt. Here, $\Delta C_{p,g}$ refers to the transition from the metallic glass to the metallic undercooled liquid, whereas ΔH_m refers to that from a crystalline mixture containing a large amount of semiconducting Si to a metallic liquid. The deviation suggests that the heat of fusion of the alloy should be corrected for the heat of transformation of Si from semiconducting to metallic crystal in order to use eq. 9 properly. Other transitions may also occur in the melt giving liquid polyamorphism [30]. For metallic glass formers this has not yet been fully proven even if a volume transition has been recently revealed by containerless undercooling in three Zr-based melts [31].

5. Conclusions

This work is devoted to the analysis of thermodynamic and dynamic properties of metallic melts in comparison with other glass formers. Using the specific heat data now available for bulk metallic

glasses, the correlation between extensive properties has been checked for the limiting cases of marginal and good glass-formers.

Simple relationships between the $\Delta S_g/\Delta C_{p,g}$ ratio and relevant temperatures for the glass have been derived and shown to correspond to those obtained with either hyperbolic or gaussian distribution of the states in the PEL of the melt. These correlations appear useful to estimate unknown quantities when the experimental determination of the specific heat is possible.

The link between thermodynamic and dynamic properties was established by posing $T_K = T_0$. Although this is debated in the literature, it has been shown that the assumption appear reasonable in the present context of available data and scatter. The usefulness of this position stems also from the strong correlation existing between T_0 and the B parameter in the VFT expression of viscosity.

The use of the Wang-Richet-Angell formula (eq. 9) has further shown that metallic glasses comply to the general behaviour of glass formers and has allowed to pinpoint exceptions due to peculiar transformations occurring either in the liquid or in the solid reference state.

The set of observations made in this work indicate that not only more accurate thermodynamic data are needed for metallic glass-formers, but also that careful search for structure modification in some specific systems will provide advances in the knowledge of such undercooled melts.

References

[1] E. Garrone, L. Battezzati, Phil. Mag. B 52 (1985) 1033-1045.
[2] C.A. Angell, Mrs Bull. 33 (2008) 1-12.
[3] G. Ruocco, F. Sciortino, F. Zamponi, C. De Michele, T. Scopigno, J. Chem. Phys. 120 (2004) 10666-10680.
[4] G. Dalla Fontana, L. Battezzati, submitted.
[5] F.H. Stillinger, P.G. Debenedetti, T.M. Truskett, J. Phys. Chem. B 105 (2001) 11809-11816.
[6] Q.K. Jiang, X.D. Wang, X.P. Nie, G.Q. Zhang, H. Ma, H.J. Fecht, J. Bendnarcik, H. Franz, Y.G. Liu, Q.P. Cao, J.Z. Jiang, Acta Mater. 56 (2008) 1785-1796.
[7] H. Tanaka, Phys. Rev. Lett. 90 (2003) 055701.
[8] I. Gallino, J. Schroers, R. Busch, J. Appl. Phys. 108 (2010) 063501.
[9] L. Battezzati, A. Castellero, P. Rizzi, J. Non-Cryst Solids 353 (2007) 3318-3326.
[10] A. Cai, X. Xiong, Y. Liu, H. Chen, W. An, X. Li, Y. Zhou, Y. Luo, Eur. Phys. J. B 64 (2008) 147-151.
[11] L. Battezzati, Rev. Adv. Mater. Sci. 18 (2008) 184-189.
[12] S. Mukherjee, J. Schroers, Z. Zhou, W.L. Johnson, W.K. Rhim, Acta Mater. 52 (2004) 3689-3695.
[13] L.W. Wang, H.J. Fecht, J. Appl. Phys. 104 (2008) 113538.
[14] S.C. Glade, R. Busch, D.S. Lee, W.L. Johnson, R.K. Wunderlich, H.J. Fecht, J. Appl. Phys. 87 (2000) 7242-7248.
[15] Z. Evenson, R. Busch, Acta Mater. 59 (2011) 4404-4415.
[16] O.N. Senkov, Phys. Rev. B 76 (2007) 104202.
[17] Z.P. Lu, Y. Li, C.T. Liu, J. Appl. Phys. 93 (2003) 286-290.
[18] M. Ikeda, M. Aniya, Intermetallics 18 (2010) 1796-1799.
[19] R. Busch, W. Liu, W.L. Johnson, J. Appl. Phys. 83 (1998) 4134-4141.
[20] Y. Kawamura, A. Inoue, Appl. Phys. Lett. 77 (2000) 1114-1116.
[21] G. Fiore, L. Battezzati, J. Alloy Compd. 483 (2009) 54-56.
[22] B.A. Legg, J. Schroers, R. Busch, Acta Mater. 55 (2007) 1109-1116.
[23] R. Mishra, K. Dubey, J. Therm. Anal. Calorim. 50 (1997) 843-856.
[24] L. Hu, X. Bian, W.H. Wang, G. Liu, Y. Jia, J. Phys. Chem. B. 109 (2005) 13737-13742.
[25] G.J. Fan, H. Choo, P.K. Liaw, J. Non-Cryst Solids. 351 (2005) 3879-3883.
[26] L.M. Wang, C.S. Angell, R. Ranko, J. Chem. Phys. 125 (2006) 074505.
[27] V.P. Privalko, J. Phys. Chem. 84 (1980) 3307-3312.
[28] V. Lubchenko, P.G. Wolynes, J. Chem. Phys. 119 (2003) 9088-9105.
[29] C.A. Angell, Science 267 (1995) 1924-1935.
[30] I.S. Voivod, P.H. Poole, F. Sciortino, Nature 412 (2001) 514-517.
[31] J.J.Z. Li, W.K. Rhim, C.P. Kim, K. Samwer, W.L. Johnson, Acta Mater. 59 (2011) 2166-2171.

Figure captions

Fig. 1. The correlation between ΔS_g, the entropy of the liquid frozen-in at the glass transition temperature and the corresponding enthalpy, ΔH_g. Both quantities are referred to the respective value at the melting (eutectic) point ΔS_m and ΔH_m. Meaning of lines is given in the text. Black and white circles refer to organic and inorganic glass formers (see supplementary information online).

Fig. 2. Plot of ΔS_g versus $\ln(T_g/T_K)$. The lines express the correlation between the quantities on the axes when a constant ΔC_p is assumed [27] with values of 17.4 J/mol·K and 12.5 J/mol·K. Numbers correspond to the alloys listed in Tab. 1.

Fig. 3. The ratio of T_K to T_0 for various glass formers as a function of the kinetic fragility parameter, *m*, as obtained with different techniques. Symbols as in Fig. 1, numbers as in Fig. 2.

Fig. 4. The $\Delta S_g/\Delta C_{p,g}$ ratio versus $(T_g - T_K)/T_K$. Symbols as in Fig. 1, numbers as in Fig. 2

Fig. 5. The $\Delta S_g/\Delta C_{p,g}$ ratio versus $(T_g - T_0)/T_0$. Symbols as in Fig. 1, numbers as in Fig. 2

Fig. 6. The correlation between the *B* parameter in the VFT equation and $(T_g - T_0)$ for the alloys listed in Table. 1. Symbols as in Fig. 1, numbers as in Fig. 2

Fig. 7. Plot of m_{calc} calculated according to eq. 9 versus the measured *m* fragility parameter for metallic glasses. The insert reports the same plot for the organic and inorganic glass formers (see supplementary information online). Symbols as in Fig. 1, numbers as in Fig. 2

Table captions:

Tab.1. List of glassy metallic alloys and their thermal properties.

Supplementary information online.

Tab. 1. List of organic and inorganic glasses and references to their thermal properties.

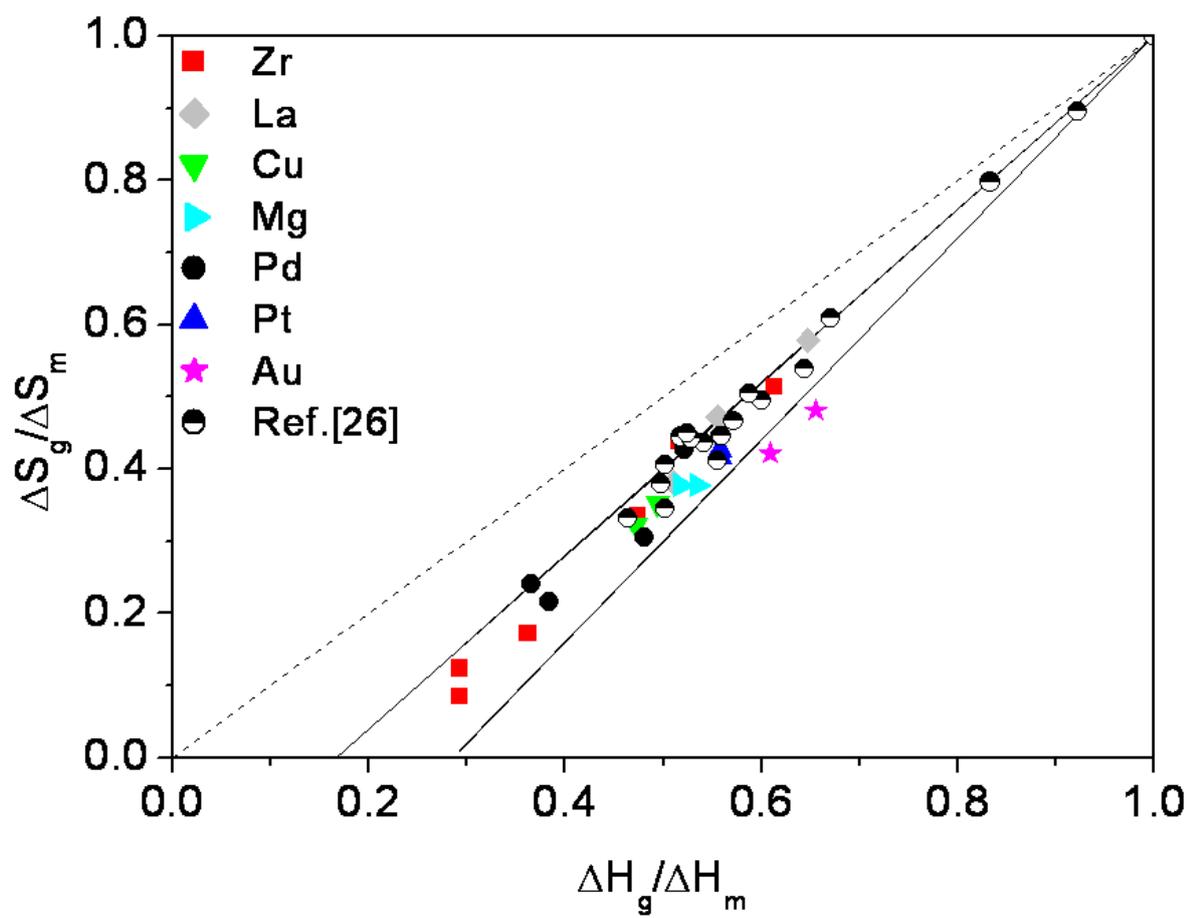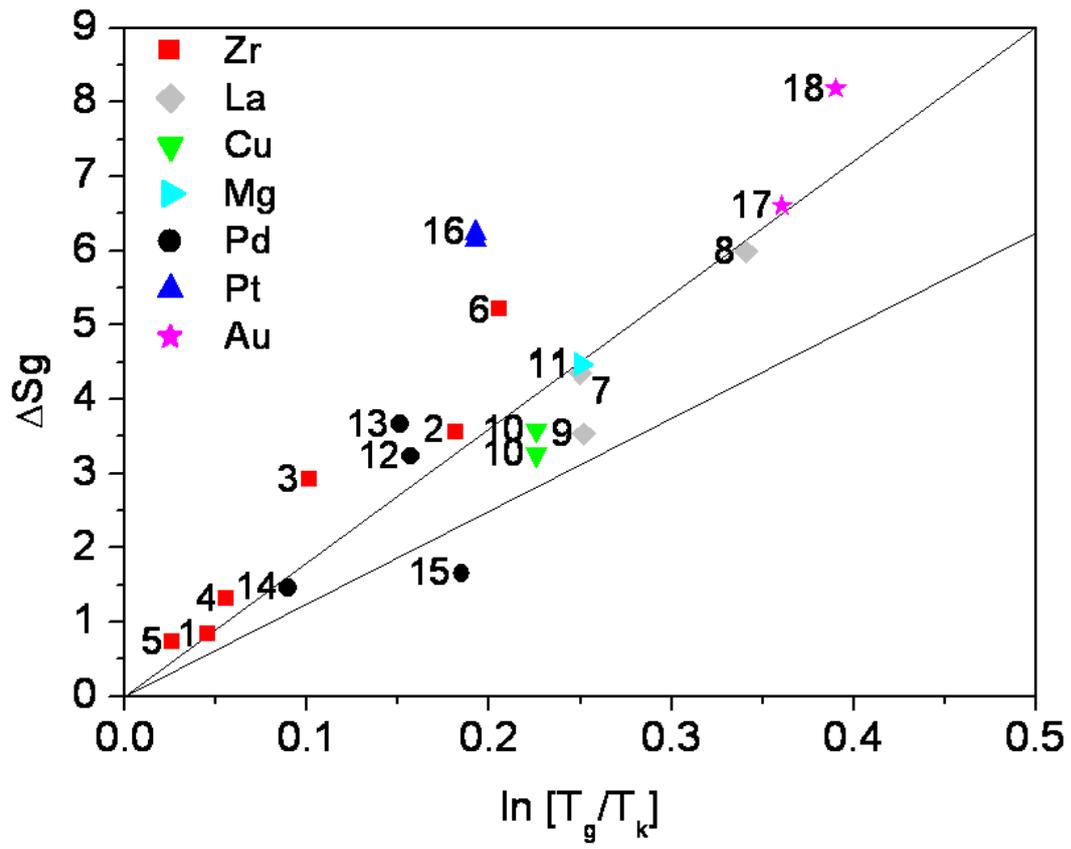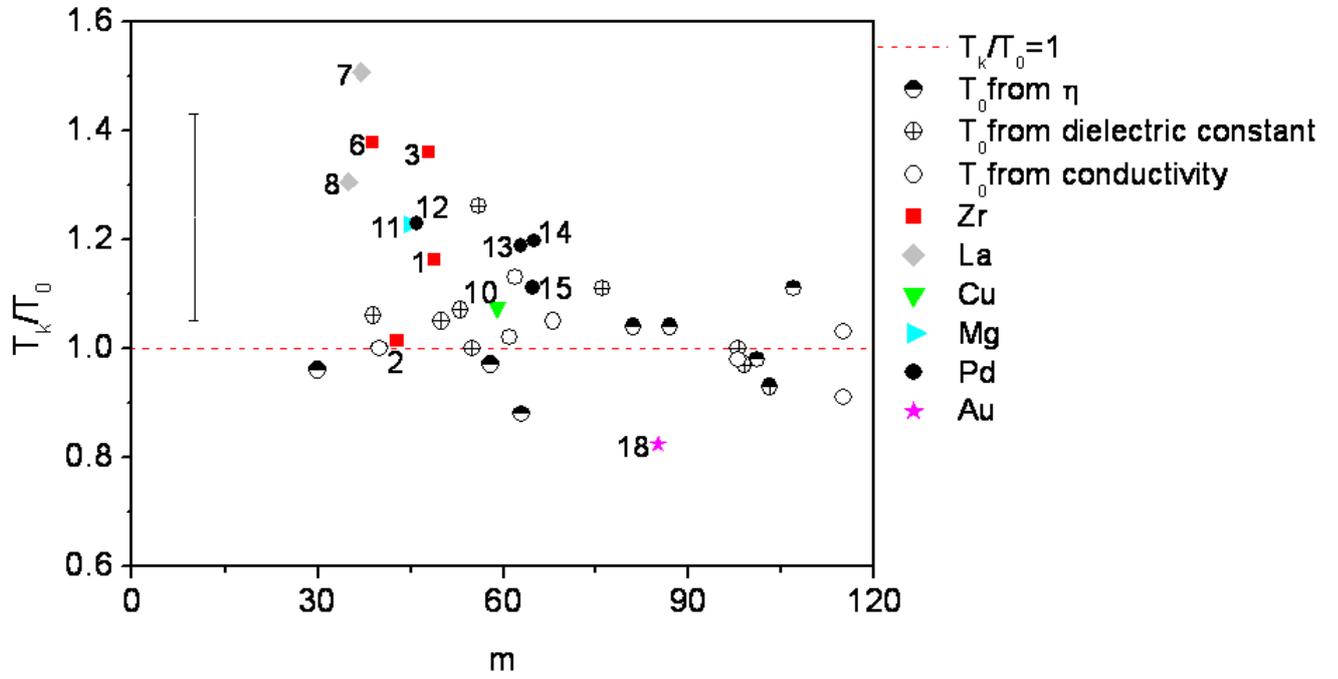|	Alloys	$T_m[K]$	$T_g[K]$	$T_k[K]$	$T_0[K]$	ΔH_m [kJ/mol]	ΔH_g [kJ/mol]	ΔS_m [J/molK]	ΔS_g [J/molK]	$\Delta C_{p,g}$ [J/molK]	m	B	Refs.
1	$Zr_{46}(Cu_{4.5/5.5}Ag_{1/5.5})_{46}Al_8$	1063	703	671	578	7,1	2,1	6,7	0,8	17,9	49		[6]
2	$Zr_{46}Cu_{46}Al_8$	979	715	596	588	8,0	4,2	8,2	3,6	16,5	43		[6]
3	$Zr_{41,2}Ti_{13,8}Cu_{12,5}Ni_{10}Be_{22,5}$	937	620	560	412 413 390 412	8,2	3,9	8,8	2,9	22,5	48	8514 8425,2 9282 7631	[7] [8-13]
4	$Zr_{52,5}Cu_{17,9}Ni_{14,6}Al_{10}Ti_5$	1072	675	638		8,2	3,0	7,7	1,3	19,8		6043,6 6044	[10, 12-14]
5	$Zr_{57}Cu_{15,4}Ni_{12,6}Al_{10}Nb_5$	1091	682	664		9,4	2,7	8,6	0,7	20,8		5929	[10, 13-14]
6	$Zr_{44}Ti_{11}Ni_{10}Cu_{10}Be_{25}$	921	620	504,5	366,6	9,3	5,7	10,1	5,1	20,0	39	9311,6	[15]
7	$La_{55}Al_{25}Cu_{10}Ni_5Co_5$	661	466	363	241,2	6,1	3,4	9,2	4,3	16,1	37	6657,1	[10, 16-17]
8	$La_{55}Al_{25}Cu_{10}Ni_{10}$	662	467	332	254,7	6,8	4,4	10,3	6,0	14,8	35	6240,2	[10, 16-17]
9	$La_{62}Al_{14}Cu_{20}Ag_4$	656	404	314	371	6,1	3,1	9,3	3,5	13,2			[6]
10	$Cu_{47}Ti_{34}Zr_{11}Ni_8$	1114	673	537	500	11,3	5,3 5,6	10,1	3,3 3,6	14,3 15,5	59	6000 8710,8	[8, 9, 10-11, 14, 18]
11	$Mg_{65}Cu_{25}Y_{10}$	730	411	320	261	8,7	4,5 4,6	11,8	4,5 4,4	14,6 16,1	45	5746 5768	[8-11, 19]
12	$Pd_{40}Ni_{40}P_{20}$	884	570	487	396	9,4	4,5	9,4	3,2	19,8	46	3600 7059 6098,4	[8-11, 13] [7, 9, 20],
13	$Pd_{40}Ni_{10}Cu_{30}P_{20}$	798	578	497	418	6,8	3,6	6,8	3,6	21,3	63	6061	[8-10]
14	$Pd_{43}Ni_{10}Cu_{27}P_{20}$	818	582	532	446	5,0	1,8	5,0	1,5	18,7	65	3675 4593,8	[8-9, 11]
15	$Pd_{77,5}Cu_6Si_{16,5}$	1015	628	560	505	7,8	3,0	7,8	1,6	14,1	65	3820	[9, 13, 21]
16	$Pt_{57,3}Cu_{14,6}Ni_{5,3}P_{22,8}$	754	480	396	336	11,4	6,4	14,7	6,1	27,8 27,1		5510,4	[8, 22]
17	$Au_{81,4}Si_{18,6}$	636	290	202		9,8	6,0	15,8	6,6	15,8			[23]
18	$Au_{77}Ge_{13,6}Si_{9,4}$	625	294	199	241,3	10,6	7,0	17,0	8,2	16,9	85		[23-25]

Fig. 1

Fig.2

Fig. 3

Fig.4

Fig. 5

Fig. 6

Fig. 7